SEISMIC SEAWALL STABILITY ON SOFT CLAY

A. B. Price[(1)], J. Ugalde[(2)], and T. Travasarou[(3)]

[(1)] *Project Engineer, Fugro, a.price@fugro.com*
[(2)] *Principal Engineer, Fugro, jugalde@fugro.com*
[(3)] *Principal Engineer, Fugro, ttravasarou@fugro.com*

Abstract

The seismic stability of a seawall founded on a deep, soft (medium sensitive) clay deposit is evaluated. Site-specific in-situ and laboratory test data, together with datasets for similar soils in the literature, are used to characterize the soft clay behaviors most important for modelling seismic seawall stability, including undrained shear strength, shear strain dependent modulus reduction and damping, cyclic strength, rates of large shear strain accumulation during undrained cyclic loading, and monotonic strain softening and brittleness. Nonlinear deformation analyses with alternative constitutive models and calibrations are used to represent the soft clay and to investigate the effects of different approximations of cyclic softening behaviors on simulated, co-seismic seawall deformations.

Commonly, post-cyclic monotonic shear tests, in combination with clay sensitivity (e.g., estimated from field vane shear test measurements), are used to define strain-dependent strength envelopes for modelling cyclic deformations in soft clay. This approach is simple and has been used in sliding block type and nonlinear deformation analyses. The appropriateness of a single strain-dependent strength envelope and its approximate representation of path dependent large strain stiffness and strength degradation behaviors depends, in general, on (1) the clay sensitivity and brittleness, (2) the shear-strain range of interest/expected degree of localization (e.g., do shear bands coalesce and form a well-defined localized failure zone, or are shear zones more diffuse?), and (3) the loading characteristics. With recent advances in available constitutive models, more emphasis can now be given to matching cyclic strengths (for both level and sloping ground conditions) and stress-strain/stress path responses from laboratory tests by explicit modelling of pore pressure generation and evolution of stiffness, fabric, and dilatancy during cyclic loading. A set of PM4Silt and UBCHYST calibrations are developed to evaluate the effect of these alternative approaches on simulated, co-seismic seawall deformations. Calibrations with monotonic strain softening (based on post-cyclic monotonic shear strength measurements) exhibited greater localization, whereas a calibration prioritizing cyclic test data developed relatively diffuse shear zones, consistent with observations from dynamic centrifuge tests in the literature for insensitive to medium sensitive soft clay embankments and slopes. Differences in soft clay modelling resulted in differences in seawall surface displacements, patterns of deformation beneath the seawall, and effectiveness of pile pinning from existing pier piles. Overall, the selection of an appropriate constitutive model and calibration approach for approximating clay-like behavior for nonlinear deformation analyses should consider: (1) the goals of the analyses, (2) the behaviors most important for estimating deformations and uncertainty in their characterization, (3) the relevant initial conditions, and (4) the loading characteristics.

Keywords: Geotechnical earthquake engineering, Nonlinear deformation analysis, Seawall, Soft clay

1. Introduction

This paper presents results from nonlinear deformation analyses used to evaluate the seismic stability of the Port of San Francisco Seawall in Yerba Buena Cove, where the seawall is founded on deep, soft bay mud (Young Bay Mud). Alternative constitutive models and calibrations were used to represent the Young Bay Mud (YBM) and to investigate the effects of different approximations of cyclic softening behaviors on simulated, co-seismic seawall deformations.

2. Geologic Setting and Construction History

The Port of San Francisco Seawall, constructed between 1879 and 1916, made possible development of the present-day San Francisco waterfront, providing flood and wave protection to Downtown San Francisco and stabilizing hundreds of acres of filled land. The seawall is located at the north-eastern tip of the San Francisco Peninsula (a 7-mile-wide peninsula dividing the Pacific Ocean from the southern San Francisco Bay) just inside the Golden Gate (a narrow opening to the bay) in a hydrologically dynamic zone where river flow and tidal current converge. The Quaternary geology of the bay is characterized by alternating glacial and interglacial stages (approximately every 100,000 years), causing fall and rise of sea level and deposition of alternating layers of sandy alluvium and estuarine mud on the bay floor. The seawall is generally founded on Holocene (the present interglacial stage) deposits of soft bay mud (Young Bay Mud) with loose sand interbeds (Young Bay Mud Sand) likely deposited from pulses of coarse sediment introduced by river flow and tidal currents.

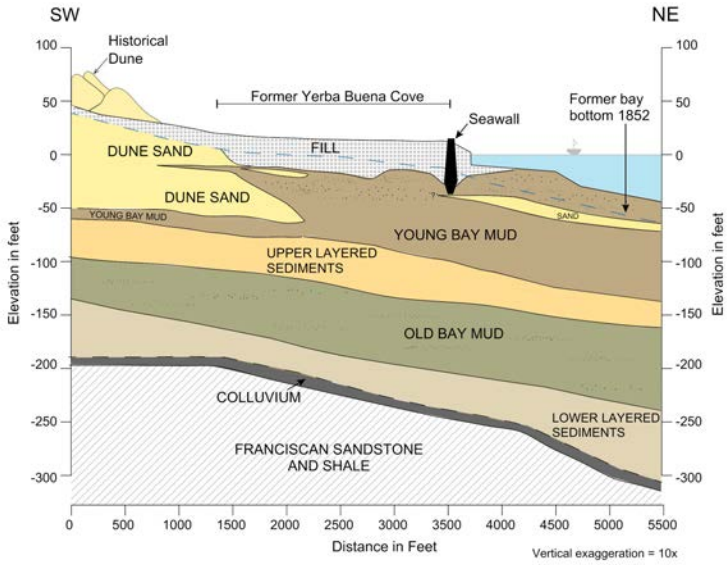

Fig. 1 – Conceptual geologic cross section in Yerba Buena Cove

The seawall was built hundreds of feet bayward of the natural shoreline by dredging an approximately 100-foot wide and 30-foot deep trench through native Young Bay Mud and filling it with rock to create a pyramid shaped dike up to 40 feet tall, capped with a bulkhead wall. Predominately loose, sandy fill was placed behind the seawall to reclaim the natural tidelands. A conceptual geologic cross section in Yerba Buena Cove, where the seawall is founded on deep YBM, is shown on Fig. 1. In Yerba Buena Cove, the deep YBM is underlain by Upper Layered Sediments (ULS) consisting of medium dense to very dense sands and stiff to very stiff clays deposited during a sea level low stand. The ULS is underlain by Old Bay Mud (OBM), a stiff to very stiff estuarine clay deposited during the Sangamon interglacial stage approximately 100,000 years ago when sea level was similar to present day. Lowered Layered Sediments (LLS) underly the

OBM and consist of estuarine, alluvial and colluvial deposits from earlier glacial cycles. The top of the Franciscan Complex bedrock is at approximately -250 feet elevation in Yerba Buena Cove.

3. Young Bay Mud Characterization

Characterization of Young Bay Mud strength, stiffness and cyclic loading behaviors is important for evaluating seismic stability of the seawall in Yerba Buena Cove. Monotonic and cyclic loading behaviors were characterized by site-specific in-situ and laboratory test data, including from cone penetration tests (CPTs), field vane shear tests (FVTs), P-S suspension logging, and laboratory direct simple shear (DSS) tests and constant rate of strain (CRS) one-dimensional consolidation tests. Pairs and triples of explorations performed at the same location were used to develop site-specific correlations between CPT measurements and engineering properties (e.g., undrained shear strength and small-strain shear modulus). These groupings of explorations also helped reduce uncertainty stemming from the limitations of any given measurement.

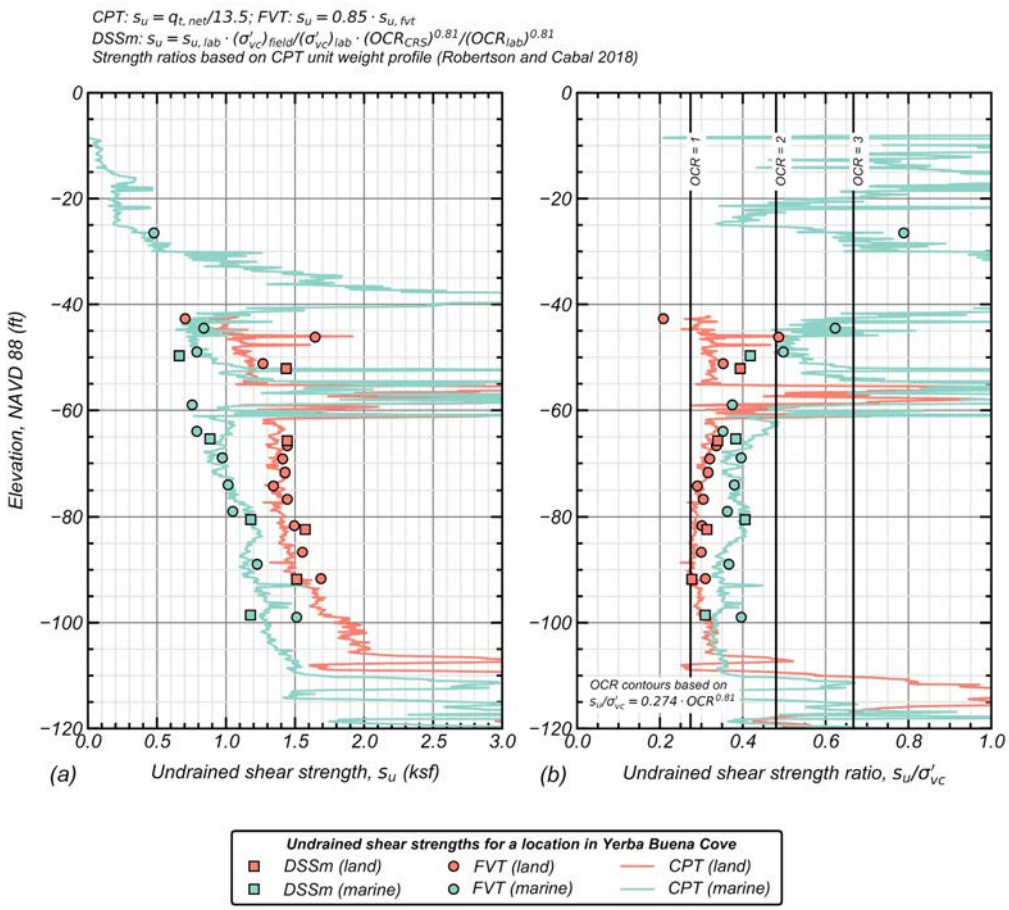

Fig. 2 – Integration of in-situ and laboratory test strength data for one location along the seawall alignment in Yerba Buena Cove: (a) undrained shear strength; (b) undrained shear strength ratio

For example, monotonic undrained shear strengths from laboratory DSS tests on high-quality piston samples, FVTs and CPTs are presented on Fig. 2 for two such groupings of explorations in Yerba Buena Cove. The red lines and markers are for explorations performed just landward of the waterfront line (land explorations) and the blue lines and markers are for explorations performed bayward of the waterfront from a pier deck (marine explorations). The DSS tests were performed following a SHANSEP (Stress History and Normalized Engineering Properties [1]) type reconsolidation method. The DSS test data points shown on Fig. 2 were adjusted for effective overburden and overconsolidation ratio (OCR) to reflect best estimate in-

situ conditions, where in-situ OCRs were estimated from CRS consolidation tests performed on specimens from the same samples as the DSS test specimens. The CRS consolidation tests were also used to evaluate sample quality based on several criteria [2, 3, 4]; overall, the quality of samples was reasonably good and similar or better than that of high-quality samples tested as part of other projects in the general vicinity. The FVT data was corrected by applying a Bjerrum [5] correction factor of 0.85 based on the plasticity of the YBM. Lastly, the CPT data is plotted for a site-specific cone factor, N_{kt}, of 13.5. In general, there is very good agreement between the three test types shown on Fig. 2. Consistency between the different tests (for both the data shown on Fig. 2 and for exploration couples/triples performed at other locations along the waterfront) reduced uncertainty in the YBM strength and allowed for reliable strength estimates in locations where only CPTs were performed. Differences in the land and marine strength profiles reflect differences in OCR and effective overburden (i.e., the land YBM is beneath an approximately 40-foot thick rock dike).

Monotonic and cyclic undrained shear strengths from DSS tests performed on YBM samples collected from multiple locations in Yerba Buena Cove are summarized on Fig. 3. Monotonic undrained shear strength ratios are plotted versus OCR on Fig. 3a for tests performed on samples collected from both land and marine explorations. The strength increase with OCR is well represented by the expression $s_u/\sigma_{vc}' = 0.274 \times OCR^{0.81}$. The normally consolidated strength ratio of 0.274 is: (1) at the higher end of the range of DSS test data for natural soft clay and silt deposits compiled by Terzaghi et al. [2], (2) greater than the value of 0.22 reported by Dames and Moore [6] for the MUNI Metro Turnaround Facility project, and (3) similar to the value (0.27) estimated by Dahl [7] based on testing of samples collected from Hamilton Air Force Base. The exponent 0.81 is similar to values measured for YBM by Dames and Moore [6] and for other soft marine clays (e.g., Ladd [8]). YBM cyclic strength data for level ground conditions (and a 3% single amplitude shear strain failure criterion) from stress-controlled undrained cyclic DSS tests are shown on Fig. 3b alongside data from the literature for different types of clay compiled by Idriss & Boulanger [9]. The YBM data is within the range of available data for other naturally deposited clays (note that the cyclic stress ratio (CSR) plotted on this figure is the cyclic shear stress divided by the monotonic undrained shear strength).

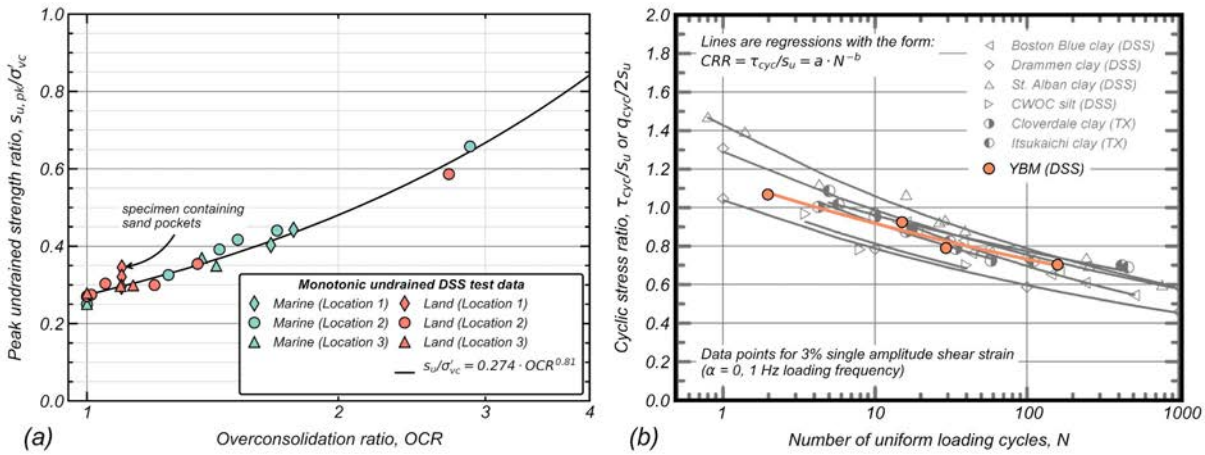

Fig. 3 – (a) YBM undrained shear strength versus OCR and (b) YBM cyclic strength

The YBM in Yerba Buena Cove near the seawall was found to have medium sensitivity and exhibit relatively ductile stress-strain responses. Sensitivity (i.e., the ratio of peak to remolded undrained shear strength) from field vane tests was approximately 4.3 on average (ranging from approximately 2.3 to 5.8). Ratios of peak to residual undrained shear strength from intact field vane tests (i.e., before remolding) were approximately 2.2 on average (ranging from approximately 1.5 to 2.7). Peak shear strengths from monotonic undrained DSS tests were reached at shear strains between approximately 3% and 7%, with mild strain-softening behaviors after approximately 10%-15% shear strain (although, post-peak stress-strain responses at larger shear strains may be affected by nonuniform stress conditions in the DSS specimens [10]). Post-cyclic undrained shear strength and stiffness degradation was also evaluated for YBM by performing undrained

monotonic shearing after cyclic loading of DSS specimens. Post-cyclic shear strengths were generally between 60% and 90% of the strength of corresponding virgin specimens, and were reached at shear strains between approximately 7% and 18% (note that the DSS specimens were recentered before post-cyclic shearing). Post-cyclic strength loss was generally greater for specimens developing greater excess pore pressures/shear strains during cyclic loading, consistent with data for other clays in the literature (e.g., Koutsoftas [11], Andersen et al. [12], and Jitno [13]). These post-cyclic strength data are summarized later.

4. Nonlinear Deformation Analyses

4.1 Seismic hazard

Seismic seawall stability was evaluated for probabilistically based, site-specific earthquake ground motions representing average return periods of 43, 100, 225, and 975 years. Outcrop ground motions were developed by spectral matching seed motions to mean uniform hazard response spectra. Seed motions were selected based on magnitude, distance, peak intensity measures, duration, velocity pulses, and spectral shape determined from deaggregation of the seismic hazard. Results for representative ground motions for 225- and 975-year return periods are presented herein for brevity. PGA and 1 second spectral accelerations (5% damping) were 0.268 g and 0.914 g for the 225-year uniform hazard response spectrum and 0.452 g and 0.387 g for the 975-year uniform hazard response spectrum.

4.2 Modelling approach and constitutive model calibration

Two-dimensional dynamic analyses were performed to evaluate seismic seawall stability using the commercial finite difference program FLAC [14]. The FLAC model stratigraphy and finite difference grid for a seawall cross section in Yerba Buena Cove are shown on Fig. 4 (note that this figure depicts an 800-foot-long section, whereas the full numerical model was 2,200 feet wide). Model zone sizes in the vicinity of the seawall were approximately 3 feet. Liquefiable soils (the onshore fill and YBM Sand) were modeled with PM4Sand version 3.1 [15] and the YBM was modeled with either UBCHYST version 5d [16] or PM4Silt version 1 [17] as described later. The rock dike, ULS Sand, and OBM where modeled with UBCHYST, the ULS Clay was modeled with PM4Silt, and the rock was modeled as elastic.

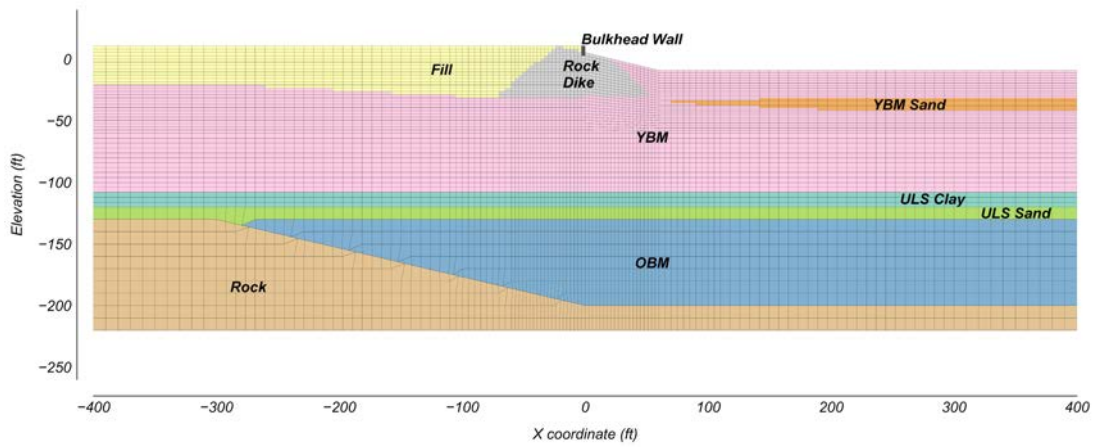

Fig. 4 – FLAC model grid and stratigraphy

The FLAC models were first initialized using elastic properties in all zones and gravity was applied in increments to allow for stress-dependent target elastic stiffnesses and densities to be updated. After elastic equilibrium was achieved, constitutive models for dynamic simulation (e.g., PM4Silt) were assigned, and the model was again brought to equilibrium. For static equilibrium solution stages, the displacements were fixed in the horizontal direction along lateral boundaries and in the vertical direction along the base of the model, and the fluid bulk modulus was set to zero. Static shear stress ratios (i.e., $\alpha = \tau/\sigma_{vc}'$) in the YBM beneath the

dike were generally between 0.1 and 0.2, decreasing with depth. Following static equilibrium, dynamic earthquake loading was simulated by applying a shear stress time history to a quiet (absorbing) boundary at the base of the model, following the procedure proposed by Mejia and Dawson [18]. Free-field boundaries were used along the lateral edges and the fluid bulk modulus was set to the bulk modulus of water; flow was not allowed during dynamic earthquake loading (i.e., locally undrained conditions). Separate analyses were performed for free-field conditions and with an existing pier. For analyses representing existing conditions, simplified pile pinning effects were modeled using linear-elastic pile and beam elements with reduced bending stiffness to account for some structural nonlinearity (e.g., cracking). Local soil-pile interaction was modeled with elastic perfectly plastic normal coupling springs (that control lateral resistance) where spring cohesion and stiffness were set based on conventional p-y spring formulations for sands [19] and clays [20].

The Young Bay Mud was modeled with either PM4Silt or UBCHYST. Analyses were performed for a set of YBM calibrations with alternative representations of cyclic softening behaviors via (1) generation of excess pore pressures and evolution of stiffness, fabric, and dilatancy during cyclic loading (based on cyclic DSS test data) and (2) monotonic strain softening (based on post-cyclic monotonic strengths and sensitivity). Calibration of PM4Silt was performed following the procedure described by Boulanger & Ziotopoulou [17]. UBCHYST parameters were calibrated to reasonably match target strain-dependent shear modulus and material damping relationships, and with a strain-dependent failure envelope implemented by a custom fish function that was evaluated for each FLAC calculation step. The alternative YBM calibrations are described as follows:

1. PM4Silt (no MSS): PM4Silt with no monotonic strain softening (MSS) (i.e., parameter $n^{b,wet} = 1$). This calibration prioritizes approximating cyclic strengths and large shear strain accumulation rates from cyclic DSS tests for sloping ground conditions. PM4Silt can approximate these behaviors through generation of excess pore pressures and evolution of stiffness, fabric, and dilatancy during undrained cyclic loading.
2. PM4Silt MSS1, MSS2, and MSS3: PM4Silt with three different rates of monotonic strain softening (i.e., parameter $n^{b,wet} < 1$). These calibrations include monotonic strain softening loosely based on post-cyclic monotonic shear strengths (for cyclic tests with sloping ground conditions). Different rates of strain softening were controlled by parameter h_{po} following a procedure used by Kiernan & Montgomery [21] to model the 1964 Fourth Avenue Landslide in Anchorage, AK. These calibrations exhibit much more brittle monotonic responses than the virgin and post-cyclic DSS lab tests.
3. UBCHYST MSS1 and MSS2: UBCHYST with two different monotonic strength envelopes/rates of monotonic strain softening based on post-cyclic monotonic shear strengths and sensitivity.

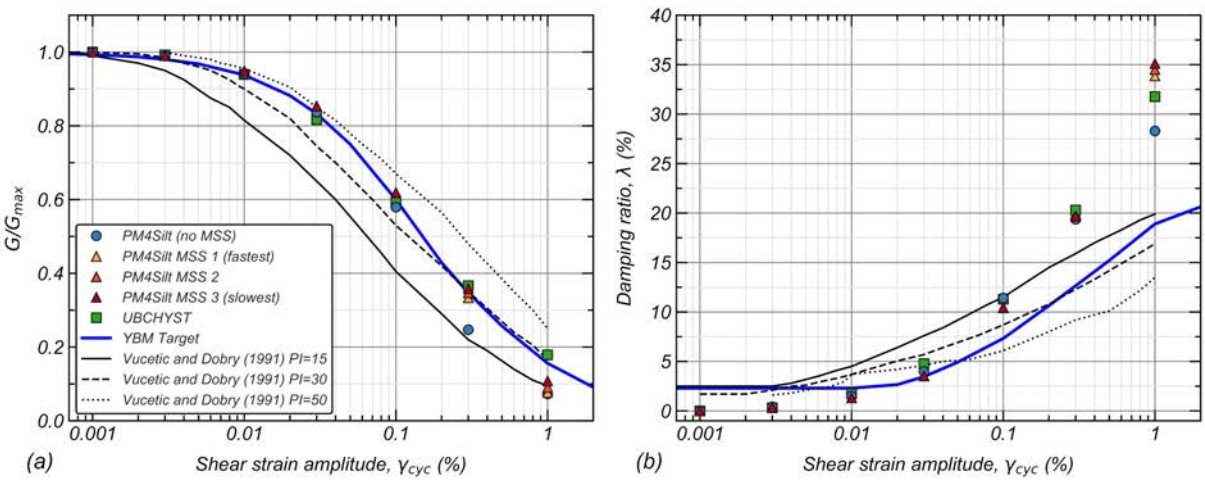

Fig. 5 – (a) Shear modulus reduction and (b) material damping (DSS simulations and target behaviors)

In all cases, stress-dependent small-strain shear modulus was assigned based on shear wave velocity (V_s) from suspension logging measurements and correlation with CPTs. The average YBM V_s was approximately 450 ft/s in the upper 30 feet of YBM beneath the rock dike. The YBM calibrations reasonably represent target modulus reduction and damping behaviors as shown on Fig. 5 (although, the simulations overdamp for symmetric loading and shear strains exceeding about 0.1%). The data points on this figure are for the third loading cycle (for a given strain amplitude) from undrained strain-controlled cyclic DSS simulations. The target relationships for YBM were developed based on available lab data which are not shown herein for brevity (i.e., resonant column, torsional shear, and DSS test data for samples collected near the seawall and for other nearby projects). The relationships by Vucetic & Dobry [22] for plasticity index (PI) of 15, 30, and 50 are shown for reference.

Monotonic shear strength envelopes and stress-strain responses for near-normally consolidated YBM (representative of conditions beneath the dike) are shown on Fig. 6. Fig. 6a presents normalized post-cyclic monotonic shear strengths from DSS tests and two alternative idealized strength envelopes that were used with UBCHYST. The idealized strength envelopes exhibit similar strength loss for shear strains less than 20%, deviating at larger shears strains with UBCHYST MSS1 plateauing at about 73% of the virgin peak strength and UBCHYST MSS2 softening to a fully remolded shear strength 25% of the virgin peak strength (i.e., a sensitivity (S_t) of 4). The UBCHYST MSS2 strength envelope was originally developed by Group Delta [23] to represent strength loss for YBM beneath the rock dike in Newmark sliding block analyses. These UBCHYST strength envelopes were selected to reasonably bound YBM softening behaviors, although selection of an appropriate strength envelope to approximate cyclic softening behaviors is difficult and depends on several factors including the clay brittleness, loading characteristics, and expected degree of localization/strain range of interest. For example, Kutter & James [24] and Park [25] observed relatively diffuse shear zones in dynamic centrifuge tests for insensitive to medium sensitive soft clay embankments and slopes, whereas static failures exhibited greater localization and distinct slip surfaces.

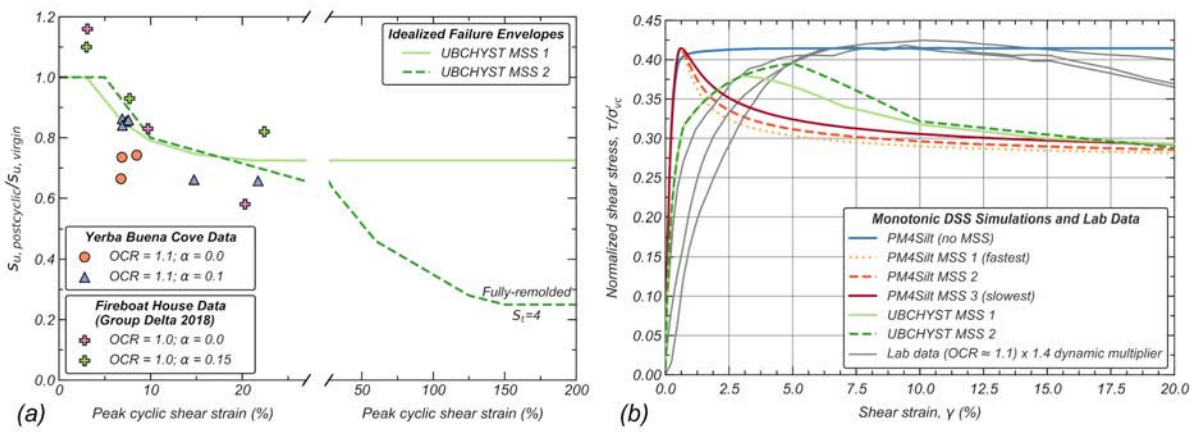

Fig. 6 – (a) Post-cyclic monotonic strength data and idealized strength envelopes and (b) simulated undrained monotonic shear responses for alternative PM4Silt and UBCHYST calibrations

Undrained monotonic DSS stress-strain responses are presented on Fig. 6b for simulations and laboratory tests. A dynamic multiplier on the undrained shear strength of 1.4 was used to account for rate effects based on (1) rapid undrained monotonic DSS tests for YBM specimens, (2) extrapolation of the level-ground CSR-N curve to one quarter cycle, and (3) available data in the literature for clays suggesting about 10% increase in undrained shear strength per log cycle increase in shear strain rate. The lab data shown on Fig. 6b has been multiplied by this factor for better comparison with the simulations. The three PM4Silt calibrations with different monotonic strain-softening rates were calibrated to plateau at 73% of the virgin peak strength (i.e., the same as the UBCHYST MSS1 strength envelope). Overall, the lab stress-strain responses are softer than the simulations and more ductile than the simulations with monotonic strain softening. All calibrations prioritize in-situ V_s data and the target shear modulus reduction curve presented

on Fig. 5 over the softer monotonic DSS response (which is known to underestimate initial stiffness [26]). While not considered in this study, alternative calibrations that better represent soft DSS responses are possible (e.g., Boulanger & Wijewickreme [27]). Monotonic strain softening in the simulations was used to partially approximate cyclic softening behaviors (e.g., post-cyclic shear strengths), hence, the simulations exhibit greater softening than laboratory monotonic DSS tests for virgin specimens.

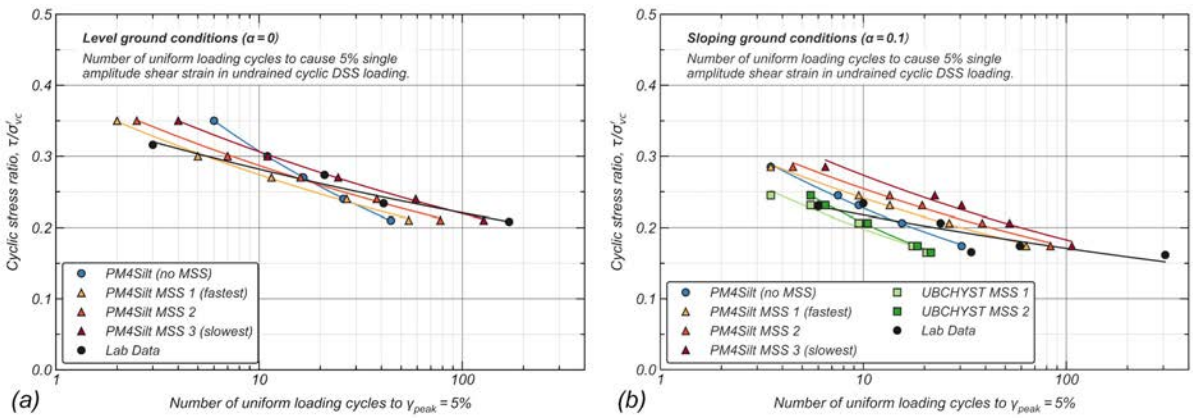

Fig. 7 – Measured and simulated cyclic strengths (5% single amplitude shear strain): (a) $\alpha = 0$; (b) $\alpha = 0.1$

Lastly, cyclic strengths for 5% shear strain in 15 uniform loading cycles from simulations and laboratory DSS tests for both level and sloping ground conditions ($\alpha = 0$ and 0.1, respectively) are shown on Fig. 7. No cyclic strength curve is shown for the UBCHYST calibrations on Fig. 7a because the model locks up (i.e., it does not continue to develop shear strains with increasing number of loading cycles) for level ground conditions and symmetric loading at CSRs that do no reach the failure envelope. Cyclic strengths and rates of large shear strain accumulation for the PM4Silt calibration with no MSS were calibrated against cyclic lab DSS test data, prioritizing behaviors for sloping ground conditions. Paramater h_{po} (the PM4Silt contraction rate parameter) was calibrated to approximate cyclic strengths for 3% and 5% shear strain and secondary parmeters (e.g, c_e and c_z) were adjusted based on comparison of stress-strain and stress-path respones with undrained cyclic DSS tests. These calibrated secondary parameters were held constant for the alternative PM4Silt calibrations (where parameters $n^{b,wet}$ and h_{po} were adjusted to produce monotonic strain softening). The UBCHYST calibrations were not adjusted based on cyclic strength or comparison with laboratory stress-strain responses from stress-controlled DSS tests (the calibration procedure only involved specification of the small-strain shear modulus, parameters controlling hysteretic behaviors, and the strength envelope, as described earlier). The PM4Silt calibrations reasonably approximate level ground cyclic strengths, whereas the calibrations with the intermediate and slowest softening rates (i.e., PM4Silt MSS 2 and MSS3) overestimate cyclic strengths for $\alpha = 0.1$ and a 5% shear strain failure criterion. Conversely, the UBCHYST calibrations underestimate cyclic strengths for $\alpha = 0.1$. The calibrations with monotonic strain softening generally exhibit faster rates of strain accumulation during undrained stress-controlled loading beyond 5% shear strain, consistent with the degree of softening for a given model/calibration.

4.3 Results from two-dimensional seawall stability analyses

The effects of the different YBM calibrations (and respective mechanisms used to approximate cyclic softening behaviors) on simulated, co-seismic seawall deformations are presented herein. Residual shear strain contours and horizontal displacement profiles for a 975-year return period ground motion, free-field conditions, and the PM4Silt calibration with no MSS are shown on Fig. 8. Shear strains are most concentrated at the base of the onshore fill and in the YBM beneath the dike. Shear strains greater than 1% develop throughout the YBM thickness beneath the bayward toe of the dike, where static shear stresses are most concentrated. This relatively diffuse shear zone is consistent with experimental observations by Kutter and James [24] and Park [25] for dynamic loading of insensitive to medium sensitive clay embankments and

slopes. Dynamic loads from vertically propagating shear waves may cause plastic deformation within a family of slip surfaces, and the competition of strain-softening and strain-rate effects may limit the degree of localization under dynamic loading conditions for these low to moderately sensitive clays (although in general, failure may eventually coalesce to a more localized shearing zone/slip surface depending on the clay brittleness and sensitivity and the loading characteristics). The direction of the offshore residual displacements away from the seawall was generally dependent on the ground motion and ground motion polarity; for this ground motion, the residual offshore displacements are negative (i.e., residual movement was towards the shore).

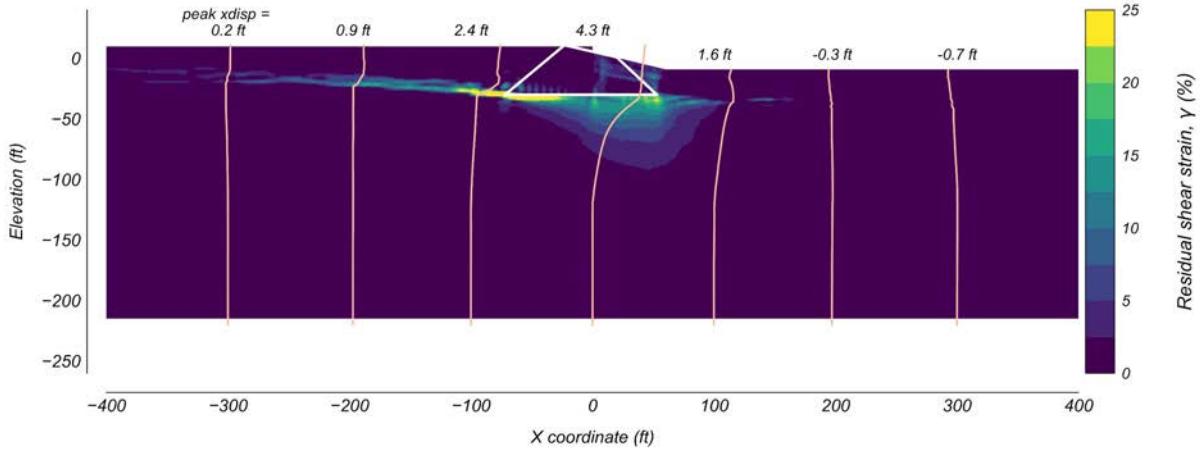

Fig. 8 – Residual shear strain contours and displacement profiles for a free-field FLAC analysis with the YBM PM4Silt calibration with no MSS and a 975-year return period ground motion

Residual horizontal displacement profiles at the waterfront line for alternative YBM calibrations are shown for free-field and existing conditions (i.e., with an existing pier) on Fig. 9 and Fig. 10, respectively. These figures present residual displacement profiles for a 225-year and a 975-year ground motion (note that the x-axis scales are different for the two return periods). For the 225-year motion and free-field conditions, all four PM4Silt calibrations exhibit similar deformations at the waterfront line, with the no MSS calibration estimating displacements 5%-10% greater than the other PM4Silt calibrations. The UBCHYST calibrations exhibit nearly identical displacements that are approximatley 40%-50% less than estimated by PM4Silt; this difference in displacements coresponds to differences in shear strain magnitude in the deeper YBM, below -60 feet elevation (~0.3% for UBCHYST and ~0.6%-1.2% for PM4Silt). For the 975-year motion and free-field conditions, the two UBCHYST calibrations bracket the surface displacement estimated by PM4Silt with no MSS. The three PM4Silt calibrations with MSS estimate surface displacements larger than UBCHYST and PM4Silt with no MSS, with greater displacement for faster softening rates. All cases with MSS exhibit greater localization within the YBM beneath the rock dike for this level of shaking compared with the no MSS case. Again, the PM4Silt calibrations estimate larger deformations within the deeper YBM (shear strains within the YBM below -60 feet elevation were approximaltey 0.5% to 1% for UBCHYST and 1% to 3% for PM4Silt with MSS for the 975-year motion and free-field conditions). This difference can be partly attributed to the following: (1) greater level ground cyclic strength for the UBCHYST calibrations and (2) observation of so-called overshooting for the UBCHYST calibrations, where a small unload-reload cycle produces an overly stiff response, limiting shear strain accumulation in the direction of the static shear stress.

Analyses including simplified pile pinning effects exhibit similar behaviors as the free-field analyses for the 225-year ground motion, with smaller displacements and rotation of the bulkhead wall. For the 975-year ground motion, pile pinning is more effective for the analyses with MSS that develop greater localization beneath the dike. Although, these analyses may overestimate pile pinning effects for the 975-year ground motion, considering that the piles were modeled using elastic elements. In any case, the PM4Silt calibrations with and without MSS produced similar magnitudes of displacement for this 975-year motion.

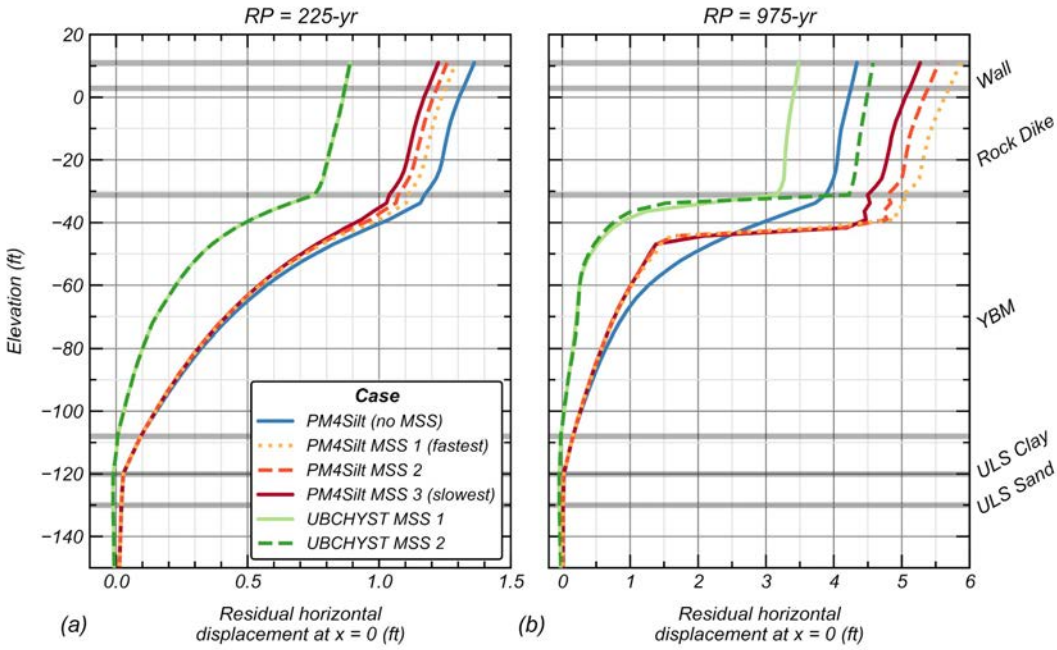

Fig. 9 – Residual displacement profiles at the waterfront line for free-field analyses with alternative YBM calibrations: (a) 225-year ground motion; (b) 975-year ground motion

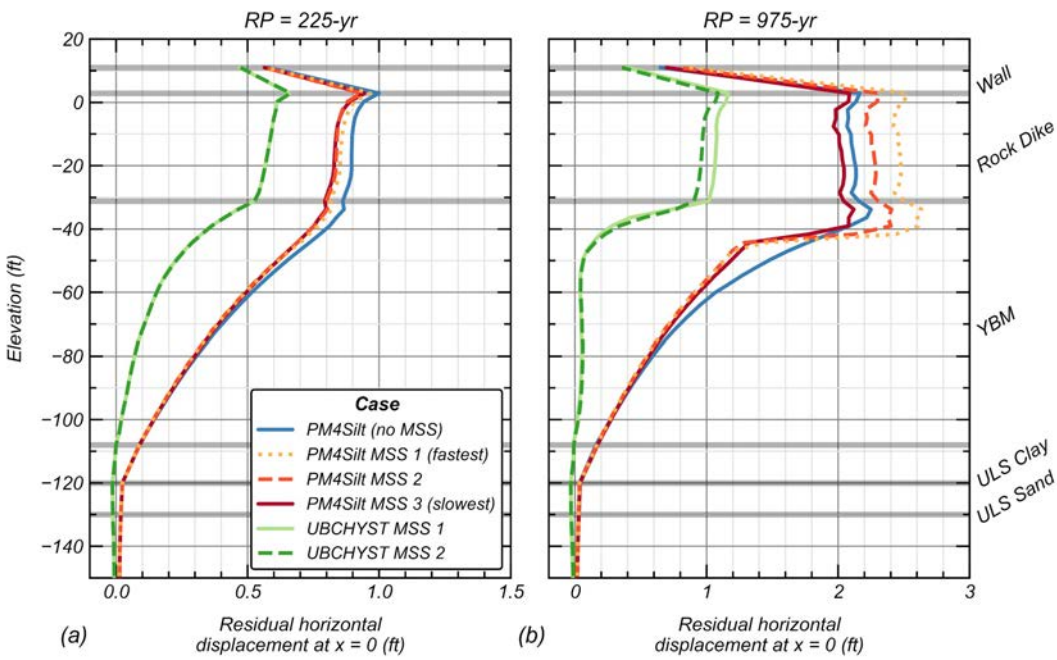

Fig. 10 – Residual displacement profiles at the waterfront line for analyses with an existing pier and alternative YBM calibrations: (a) 225-year ground motion; (b) 975-year ground motion

5. Summary and Conclusions

Nonlinear deformation analyses were used to evaluate seismic stability of the Port of San Francisco Seawall in Yerba Buena Cove, where the seawall is founded on deep YBM. Alternative calibrations and two

constitutive models were used to represent the YBM and to investigate the effects of different approximations of cyclic softening behaviors on simulated, co-seismic seawall deformations. Overall, calibrations with MSS exhibited greater localization in the YBM directly beneath the rock dike, whereas the PM4Silt calibration with no MSS and prioritizing cyclic DSS test data developed relatively diffuse shear zones. Co-seismic seawall displacements were similar (within approximately 10%) for the PM4Silt calibrations (with and without MSS) and the 225-year ground motion, whereas seawall displacements for simulations with UBCHYST were approximately 40% to 50% less (this difference is partly attributed to so-called overshooting observed in the UBCHYST simulations and differences in level ground cyclic strength). For this level of shaking (and free-field conditions), peak residual shear strains in the YBM at the waterfront line ranged from approximately 2.8% to 3.6% and differences in monotonic strain softening behavior (for a given constitutive model) had little effect on seawall displacements. For the 975-year ground motion and free-field conditions, the UBCHYST calibrations with different strain-dependent strength envelopes bracketed the displacement simulated using the PM4Silt calibration with no MSS. For this level of shaking (and free-field conditions), peak residual shear strains in the YBM at the waterfront line ranged from approximately 15% for the PM4Silt calibration with no MSS to nearly 100% for UBCHYST MSS2 (i.e., the calibration that softens to a remolded shear strength). Pile pinning (modeled in a simplified way with elastic elements with reduced section modulus) was more effective for calibrations with MSS that produced greater localization in the YBM just beneath the dike.

These analyses demonstrate how different representations of cyclic softening behaviors for a medium sensitive, ductile soft clay affect the magnitude and pattern of simulated, co-seismic seawall deformations. Alternative constitutive models and calibration approaches can be used to capture some epistemic uncertainty in these types of analyses and are useful for establishing a range of reasonable responses, although in this case the PM4Silt calibration with no MSS was considered to best represent the YBM for the relevant range of initial conditions, shaking levels, and deformations. This calibration prioritized cyclic strengths and large strain accumulation rates from cyclic DSS lab tests for the sloping ground conditions beneath the dike. Conversely, for more brittle silts and clays and levels of shaking that may result in remolding (e.g., response of the Anchorage silty clay in the Fourth Avenue landslide [21]), deformations may be reasonably estimated with models where monotonic strain softening is the primary mechanism of large shear strain accumulation. For the seismic seawall stability analyses presented herein, differences in the constitutive model and calibration used to represent the YBM had a more significant effect on simulated deformations than other reasonable parameter variations (e.g., for s_u and V_s). Differences in YBM modelling resulted in differences in both surface displacements and deformation patterns, which can impact the estimated effectiveness of existing structural elements and/or evaluation of retrofit/mitigation options. Overall, the selection of an appropriate constitutive model and calibration approach for approximating clay-like behavior for nonlinear deformation analyses should consider: (1) the goals of the analyses, (2) the behaviors most important for estimating deformations and uncertainty in their characterization, (3) the relevant initial conditions, and (4) the loading characteristics.

6. Acknowledgements

We would like to thank the Port of San Francisco and especially Steven Real (POSF Seawall Project Manager) for his leadership and unwavering support of this work. Fugro's geologists Janet Sowers and Kelly Shaw clarified the geologic setting and Fugro's Deron van Hoff coordinated the site investigation program. Comments and suggestions from Matt Wickens, Nason McCullough and the independent peer review panel of Shah Vahdani, Steve Dickenson, Jonathan Bray and Mark Salmon improved the quality of this work.

7. References

[1] Ladd, C.C., & Foott, R. (1974). New design procedure for stability of soft clays. *J. Geotech. Eng. Div.*, *100*(7), 763-786.

[2] Terzaghi, K., Peck, R.B., & Mesri, G. (1996). *Soil mechanics in engineering practice*. John Wiley & Sons.

[3] Lunne, T., Berre, T., & Strandvik, S. (1997). Sample disturbance effects in soft low plastic Norwegian clay. *Proc., Int. Symp. on Recent Developments in Soil and Pavement*, 81–103.

[4] DeJong, J.T., Krage, C.P., Albin, B.M., & DeGroot, D.J. (2018). Work-based framework for sample quality evaluation of low plasticity soils. *J. Geotech. Geoenviron. Eng., 144*(10), 04018074.

[5] Bjerrum, L., (1973). Problems of soil mechanics and construction on soft clays. *Proc., 8th Int. Conf, on Soil Mechanics and Foundation Eng.*, Moscow.

[6] Dames & Moore (1986). Factual report, site investigation, MUNI Metro Turnaround Facility, Volume I, prepared for Bechtel National, Inc., January 31, 1986.

[7] Dahl, K.R. (2011). *Evaluation of Seismic Behavior of Intermediate and Fine-Grained Soils*. Ph.D. thesis, Univ. of California, Davis.

[8] Ladd, C.C. (1991). Stability evaluation during staged construction. *J. Geotech. Eng.,* 117(4), 540-615.

[9] Idriss, I.M., & Boulanger, R.W. (2008). *Soil liquefaction during earthquakes*. EERI.

[10] DeGroot, D.J., Germaine, J.T., & Ladd, C.C. (1994). Effect of nonuniform stresses on measured DSS stress-strain behavior. *J. Geotech. Eng., 120*(5), 892-912.

[11] Koutsoftas, D.C. (1978). Effect of cyclic loads on undrained strength of two marine clays. *J. Geotech. Eng. Div., 104*(5), 609-620.

[12] Andersen, K H., Rosenbrand, W.F., Brown, S.F., & Pool, J.H. (1980). Cyclic and static laboratory tests on Drammen clay. *J. Geotech. Eng. Div.*, *106*(5), 499-529.

[13] Jitno, H. (1990). *Stress-strain and strength characteristics of clay during post-cyclic monotonic loading*. MASc thesis, The Univ. of British Columbia.

[14] Itasca Consulting Group Inc. (Itasca). (2016). FLAC User's Guide. Version 8.0. Minneapolis, MN.

[15] Boulanger, R.W., & Ziotopoulou, K. (2017). PM4Sand (version 3.1): A sand plasticity model for earthquake engineering applications. Report No. UCD/CGM-17/01. Davis, CA.

[16] Naesgaard, E., Byrne, P.M., & Amini, A. (2015). *Hysteretic model for non-liquefiable soils (UBCHYST5d).*

[17] Boulanger, R.W., & Ziotopoulou, K. (2018). PM4Silt (Version 1): a silt plasticity model for earthquake engineering applications. Report No. UCD/CGM-18/01. Davis, CA.

[18] Mejia, L.H., & Dawson, E.M. (2006). Earthquake deconvolution for FLAC. *Proc. 4th Int. FLAC Symposium*, 4-10.

[19] American Petroleum Institute (API). (2011). Geotechnical and Foundation Design Considerations. ANSI/API Recommended Practice 2GEO. 1st Ed. April.

[20] Matlock, H. (1970). Correlation for design of laterally loaded piles in soft clay. *Proc., Offshore Tech. Conf.*, 577-594.

[21] Kiernan, M., & Montgomery, J. (2020). Numerical Simulations of Fourth Avenue Landslide Considering Cyclic Softening. *J. Geotech. Geoenviron. Eng., 146*(10), 04020099.

[22] Vucetic, M., & Dobry, R. (1991). Effect of soil plasticity on cyclic response. *J. Geotech. Eng., 117*(1), 89-107.

[23] Group Delta. (2018). *Geotechnical Report New Fireboat House at Port of San Francisco Piers 22.5 and 24 San Francisco, California*.

[24] Kutter, B.L., & James, R.G. (1989). Dynamic centrifuge model tests on clay embankments. *Geotechnique*, *39*(1), 91-106.

[25] Park, D.S. (2011). *Strength loss and softening of sensitive clay slopes*. Ph.D. thesis, Univ. of California, Davis.

[26] Lunne, T., Berre, T., Andersen, K.H., Strandvik, S., & Sjursen, M. (2006). Effects of sample disturbance and consolidation procedures on measured shear strength of soft marine Norwegian clays. *Can. Geotech. J., 43*(7), 726-750.

[27] Boulanger, R.W., & Wijewickreme, D. (2019). Calibration of a constitutive model for the cyclic loading response of Fraser River Delta Silt. *Proc., 7th Int. Conf. on Earthquake Geotech. Eng.,* 121-137.

